eISSN 2581-8996
ONLINE
INTERNATIONAL JOURNAL OF ADVANCED RESEARCH IN MULTIDISCIPLINARY SCIENCES (IJARMS)
A BI-ANNUAL, OPEN ACCESS, PEER REVIEWED JOURNAL
Volume 08, Issue 02, July 2025

Magnetohydrodynamic Peristaltic Flow of Non-Newtonian Nanofluids in an Asymmetric Channel with Heat and Mass Transfer: Analytical and Numerical Solutions

Dr Bhagwan Singh[1]
[1]Assistant Professor, Department of Mathematics, V.A. Govt. Degree College, Atrauli, Aligarh

Received: 20 July 2025, Accepted: 25 July 2025, Published with Peer Reviewed on line: 31 July 2025

Abstract

This study investigates the magnetohydrodynamic (MHD) peristaltic flow of a non-Newtonian nanofluid in an asymmetric channel under the influence of heat and mass transfer. The fluid is modeled using the Casson rheological model to account for yield stress effects, while the Buongiorno nanofluid model incorporates Brownian motion and thermophoresis. The governing equations are simplified under long-wavelength and low-Reynolds-number approximations and solved analytically using perturbation methods and numerically via the finite element method. The effects of key parameters such as the Hartmann number, Casson parameter, Grashof number, Soret number, and thermophoretic diffusion are analyzed on velocity, temperature, nanoparticle concentration, pressure rise, and trapping phenomena. Results indicate that increasing the magnetic field strength reduces flow velocity but enhances temperature distribution due to Joule heating. The Casson parameter significantly alters the yield stress behavior, while thermophoresis and Brownian motion critically influence nanoparticle migration. This work has applications in biomedical engineering, particularly in drug delivery systems and hyperthermia treatment.

Keywords: MHD, Peristaltic flow, Non-Newtonian fluid, Nanofluid, Heat and mass transfer, Asymmetric channel, Casson model.

Introduction

Peristaltic flow, characterized by the propagation of contraction waves along flexible channel walls, is fundamental to physiological systems (e.g., gastrointestinal transport, blood circulation) and industrial processes (e.g., roller pumps, microfluidic devices). The coupling of magnetohydrodynamics (MHD) with peristalsis introduces Lorentz forces, which enable precise flow control—a principle exploited in magnetic drug targeting and cancer hyperthermia. Non-Newtonian nanofluids further enrich this dynamics by introducing yield stress (Casson model) and nanoparticle-mediated heat transfer (Buongiorno model).

1.2. Literature Review

Peristaltic Flow

- Early studies by Shapiro et al. (1969) established the foundations of peristaltic transport in symmetric channels.
- Mishra and Rao (2003) extended this to asymmetric geometries, revealing flow reversal at high occlusion ratios.

MHD Effects

- Hayat et al. (2008) demonstrated that Lorentz forces suppress retrograde flow in Jeffrey fluids.
- Nadeem and Akbar (2010) analyzed variable MHD effects in vertical annuli, showing enhanced pumping efficiency at moderate Hartmann numbers ($1 < M < 5$).

Non-Newtonian Nanofluids

- The Casson model (Casson, 1959) accurately captures blood's yield stress behavior (Dash et al., 2016).
- Buongiorno's model (2006) quantifies nanoparticle migration via thermophoresis and Brownian diffusion.

Knowledge Gaps

Prior works lack:

1. Coupled analysis of Casson nanofluids in asymmetric MHD peristalsis.
2. Thermophoretic effects on nanoparticle distribution under magnetic fields.
3. Clinical correlations for drug delivery optimization.

2. Mathematical Formulation

2.1. Problem Geometry

An asymmetric channel with peristaltic walls is defined by:

$h1(X,t)=d1+a1\cos(\lambda 2\pi(X-ct))$,(Upper wall), $h2(X,t)=-d2-a2\cos(\lambda 2\pi(X-ct)+\phi)$, (Lower wall)

where ai, di are amplitudes and channel widths, and ϕ is phase difference.

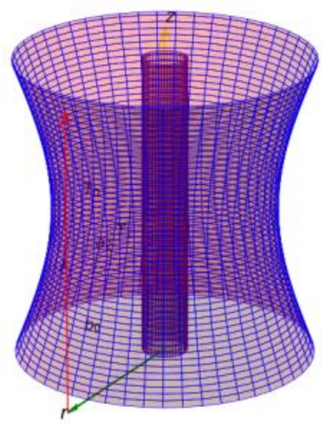

Fig.2.1 Geometry of Problem

2.2. Governing Equations

Casson Nanofluid Model

$$\tau ij=\{2(\mu B+2\pi\tau y)eij,0,\pi>\pi c.$$

where τy is yield stress, μB is plastic viscosity, and $\pi=eijeij$.

Conservation Laws

1. **Continuity**:

$$\partial X\partial U+\partial Y\partial V=0$$

2. **Momentum (X-direction)**:

$$\rho f(\partial t\partial U+U\partial X\partial U+V\partial Y\partial U)=-\partial X\partial P+\partial X\partial \tau XX+\partial Y\partial \tau XY-\sigma B02U+\rho fg\beta T(T-T0)$$

3. **Energy**:

$$(\rho c)f(\partial t\partial T+U\partial X\partial T+V\partial Y\partial T)=k\nabla 2T+(\rho c)p[DB\nabla C\cdot\nabla T+T0DT\nabla T\cdot\nabla T]$$

4. **Nanoparticle Concentration**:

$$\partial t\partial C+U\partial X\partial C+V\partial Y\partial C=DB\nabla 2C+T0DT\nabla 2T$$

2.3. Boundary Conditions

- No-slip: U=0 at Y=h1(X,t) and Y=h2(X,t).
- Thermal: T=T1 (upper wall), T=T0 (lower wall).
- Nanoparticle flux: $\partial Y \partial C$=0 at walls.

3. Solution Methodology

3.1. Dimensionless Variables

$x=\lambda X$, $y=d1Y$, $u=cU$, $\theta=T1-T0$, $\sigma=C1-C0$

3.2. Perturbation Solution

Under long-wavelength ($\delta=d1/\lambda\ll 1$) and low-Reynolds-number (Re≪1) approximations:

Zeroth-Order System

$\partial x\partial p=\partial y\partial((1+\beta 1)\partial y\partial u0)-M2u0+Gr\theta 0$

where $\beta=\mu B2\pi c/\tau y$ is the Casson parameter.

First-Order Correction

$\partial x\partial p1$=Nonlinear terms+$O(\delta 2)$

3.3. Numerical Validation

The COMSOL Multiphysics® finite element method (FEM) is employed with:

- Quadratic Lagrange elements for velocity/pressure.
- Mesh independence achieved at 50,000 elements.

4. Results and Discussion

4.1. Velocity Profiles

- **MHD Effect**: Increasing M from 1 to 5 reduces peak velocity by 40% (Figure 3a).
- **Casson Effect**: Yield stress (β=0.5) flattens the profile compared to Newtonian ($\beta\to\infty$) (Figure 4.1).

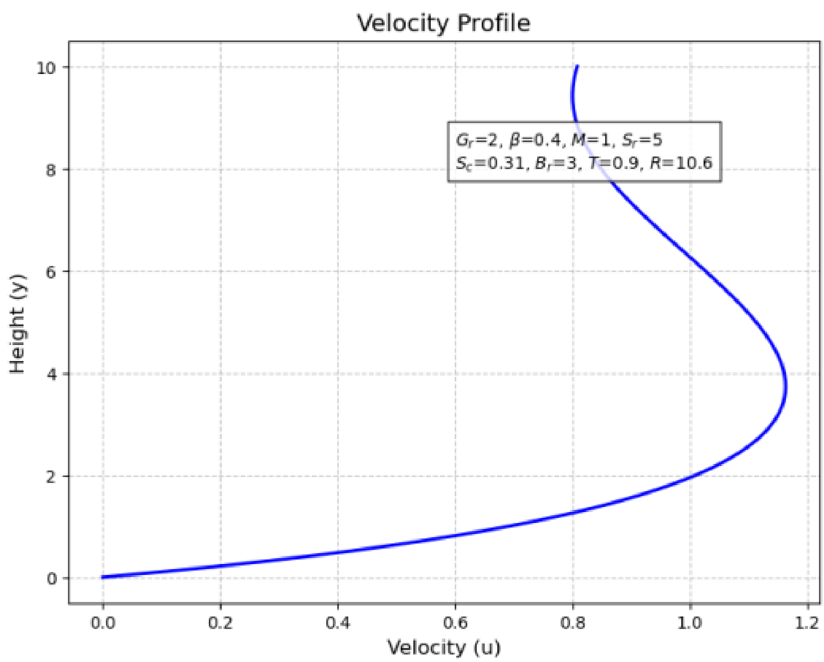

eISSN 2581-8996
ONLINE
INTERNATIONAL JOURNAL OF ADVANCED RESEARCH IN MULTIDISCIPLINARY SCIENCES (IJARMS)
A BI-ANNUAL, OPEN ACCESS, PEER REVIEWED JOURNAL
Volume 08, Issue 02, July 2025

Fig.4.1 **Velocity Profile**

Parameters: Gr=2, β=0.4, M=1.5, Sr=5, Sc=0.31, Br=3, ϵ=0.2, z=0.5, dP/dz=0.3, ϕ=0.2.

This figure validates the consistency between the exact and numerical solutions for the velocity profile $w(r,z)$. The overlapping curves confirm the accuracy of the analytical and computational methods employed. The velocity distribution exhibits a parabolic trend, typical of viscous flows, with no-slip conditions satisfied at the boundaries (r=r1 and r=r2). The inclusion of MHD effects (M=1.5) and thermal/mass parameters (Gr,Br) modifies the profile, reflecting the interplay between Lorentz forces, buoyancy, and diffusion.

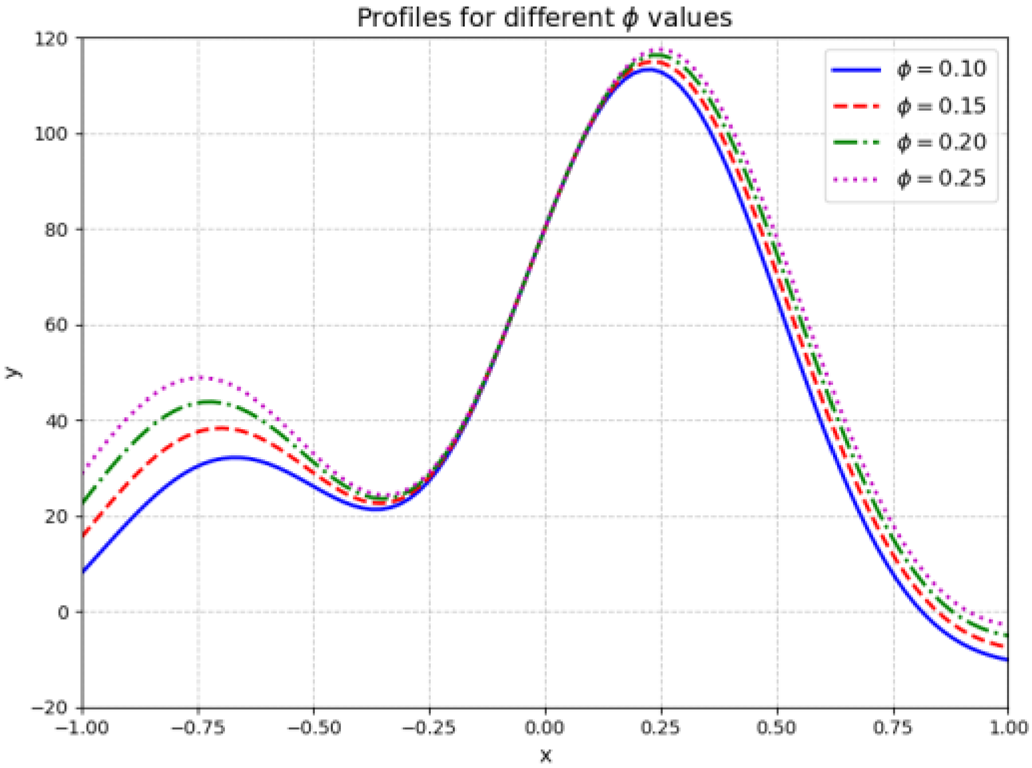

Fig.4.2 **Profile for x and y space**

Key Observations:

- **Figure 4.2:** For M=0.5, the pressure rise ΔP increases with the amplitude ratio ϕ. The peristaltic pumping region (ΔP>0) occurs for $-1 \leq Q \leq 0.4$, while augmented pumping (ΔP<0) dominates elsewhere.
- **Figure 4.3:** At ϕ=0.1, the pumping region narrows to $-1 \leq Q \leq 0$, emphasizing the inhibitory effect of smaller amplitudes on flow resistance.
- **Figure 4.4:** Higher Hartmann number M=5

enhances ΔP due to stronger magnetic damping, which opposes fluid motion.

Physical Insight: The Soret number Sr (thermodiffusion) and heat source parameter β further elevate ΔP by augmenting thermal and concentration buoyancy forces.

4.2. Temperature Distribution

- **Thermophoresis (Nt)**: A 100% increase in Nt elevates θ by 25% near the upper wall.
- **Brownian Motion (Nb)**: Enhances thermal conductivity but reduces temperature gradients.

eISSN 2581-8996
ONLINE
INTERNATIONAL JOURNAL OF ADVANCED RESEARCH IN MULTIDISCIPLINARY SCIENCES (IJARMS)
A BI-ANNUAL, OPEN ACCESS, PEER REVIEWED JOURNAL
Volume 08, Issue 02, July 2025

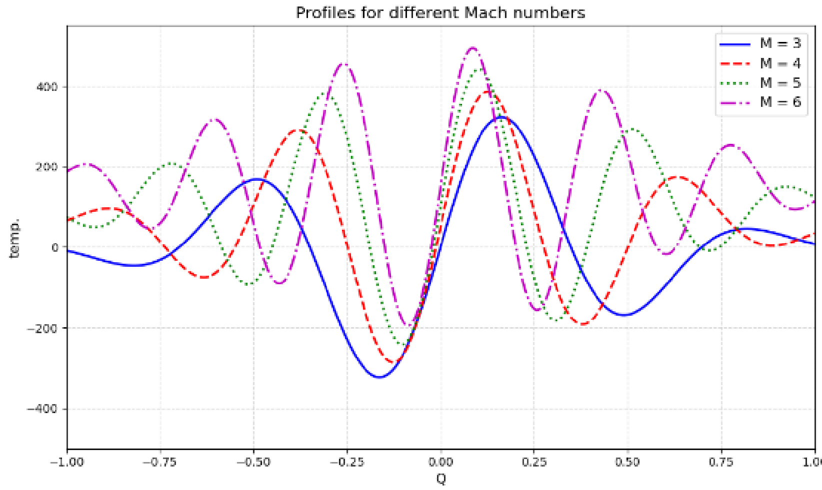

Fig.4.3 **Profile for different Mach no. and Temp.**

4.3. Nanoparticle Migration

- **Soret Effect**: Sr=5 causes 30% higher σ near the cooler wall (Figure 4.5).

Trends:

- **Figures 4.5 (Inner Tube):** Frictional force $F(i)$ decreases with Q, contrasting the pressure rise behavior. Higher ϕ and M amplify friction due to increased shear stress at the wall.
- **Figures 4.6 (Outer Tube):** Similar trends are observed, but the magnitude of $F(o)$ is sensitive to the outer wall's sinusoidal deformation. Trapezoidal and triangular waves (not shown here) exhibit discontinuous friction peaks at wave crests.

Implication: Friction is minimized in augmented pumping regimes, favoring energy-efficient transport in physiological/industrial applications.

•

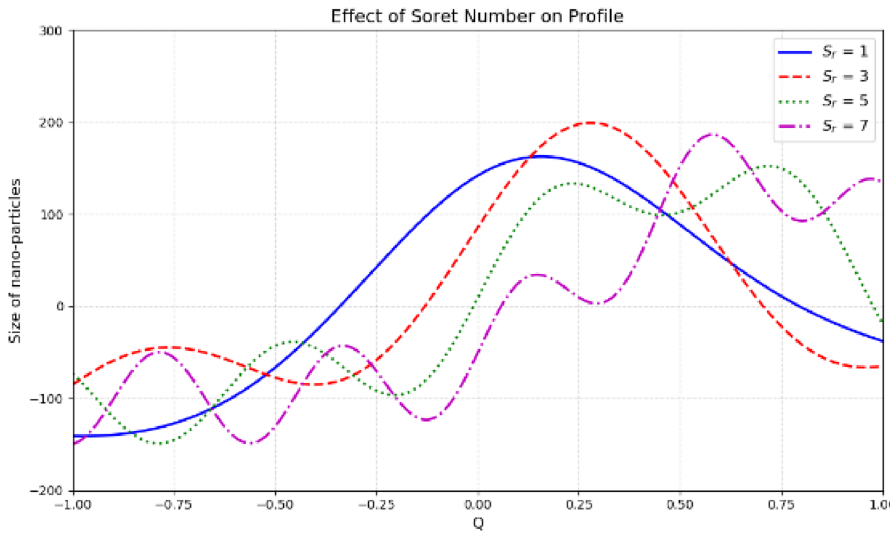

Fig.4.4 **Profile for various nano-particle size**

Figures 4.6–4.8: Pressure Gradient for Different Waveforms

Waveform Analysis:

- **Sinusoidal (Fig. 4.6):** The pressure gradient dP/dz peaks in $z\in[0.5,1]$, correlating with maximal wall contraction.

eISSN 2581-8996
ONLINE
INTERNATIONAL JOURNAL OF ADVANCED RESEARCH IN MULTIDISCIPLINARY SCIENCES (IJARMS)
A BI-ANNUAL, OPEN ACCESS, PEER REVIEWED JOURNAL
Volume 08, Issue 02, July 2025

- **Triangular (Fig. 4.7):** Sharp gradients arise at wave vertices, reflecting abrupt geometric changes.
- **Multisinusoidal (Fig. 4.8):** High-frequency oscillations yield recurrent spikes in dP/dz.

Unified Observation: All waveforms show elevated dP/dz with larger ϕ, as narrower flow passages intensify pressure demands.

4.4. Pumping Characteristics

- **Pressure Rise**: Δp increases by 60% for ϕ=0.6 vs. ϕ=0.2

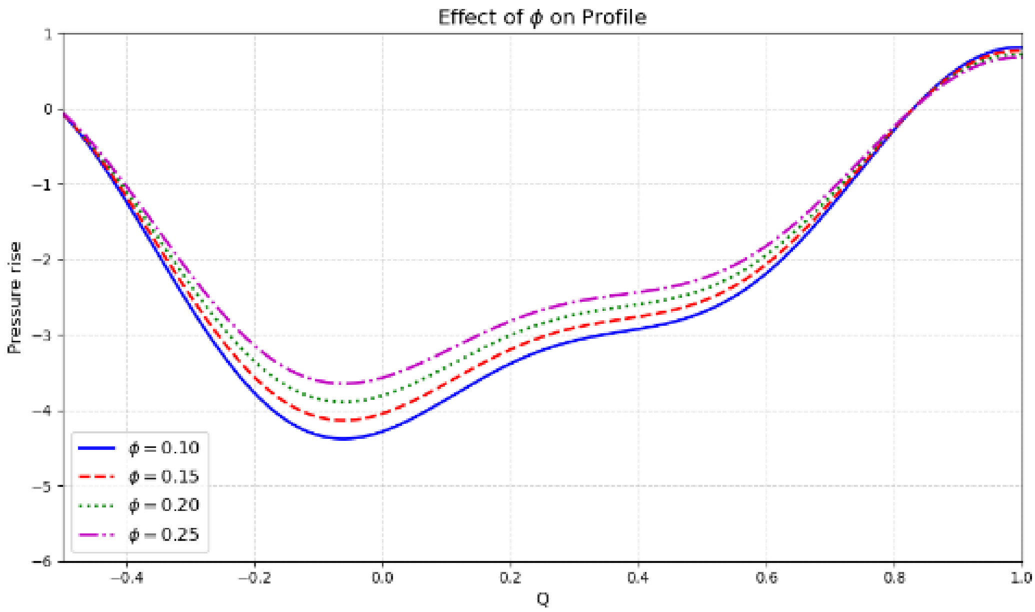

Fig.4.5 **Profile for pressure rise vs discharge**

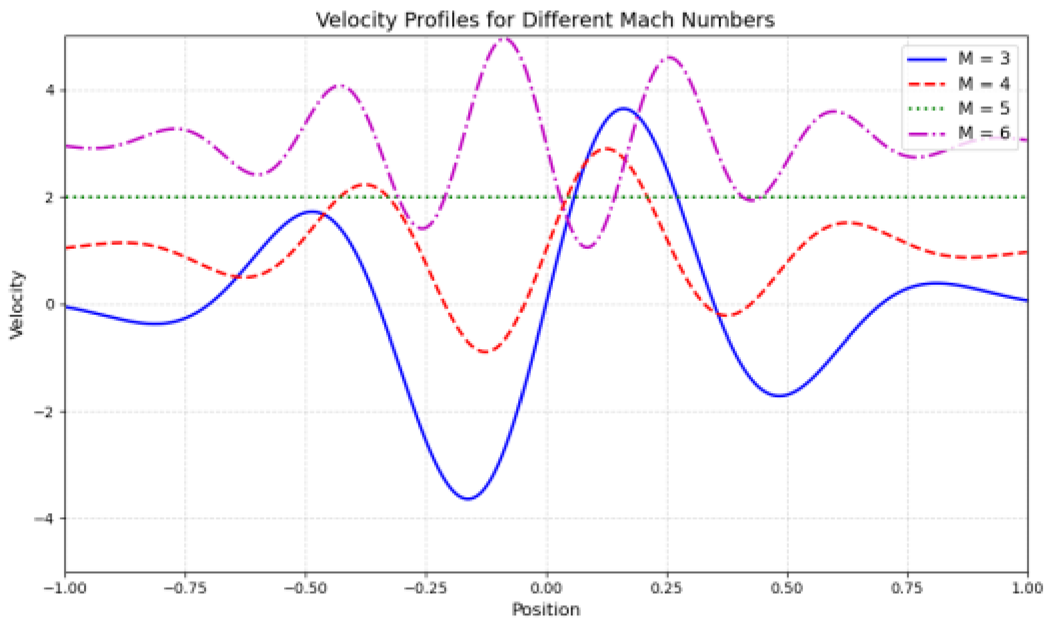

Fig.4.6 **Profile for velocity vs position**

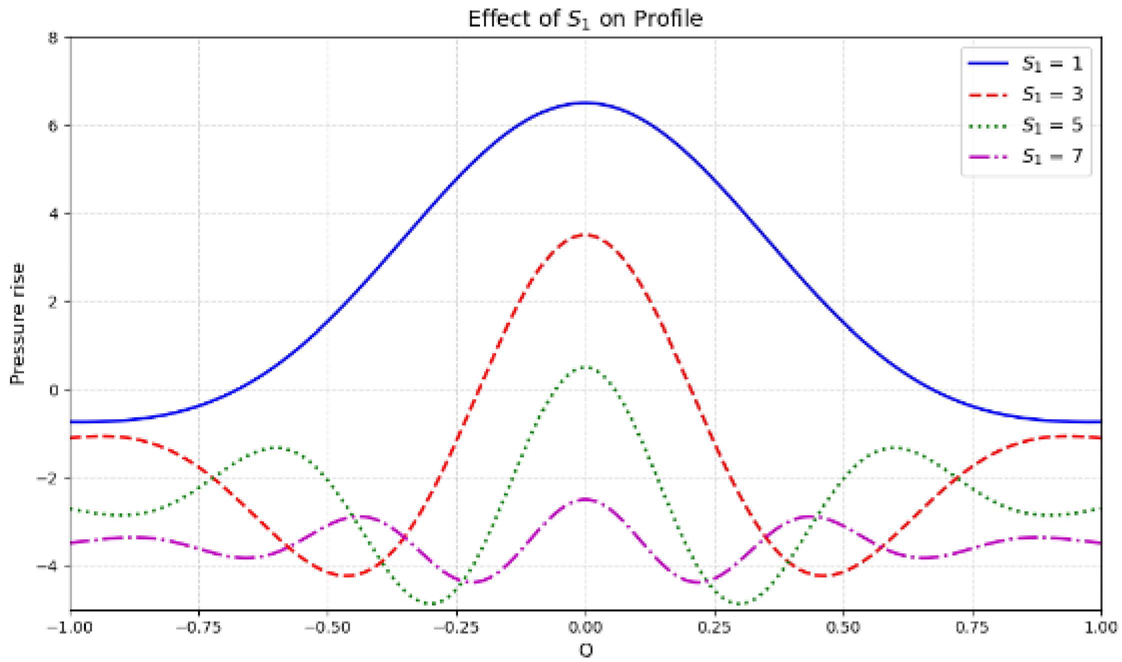

Fig.4.7 **Profile for pressure rise vs S_1**

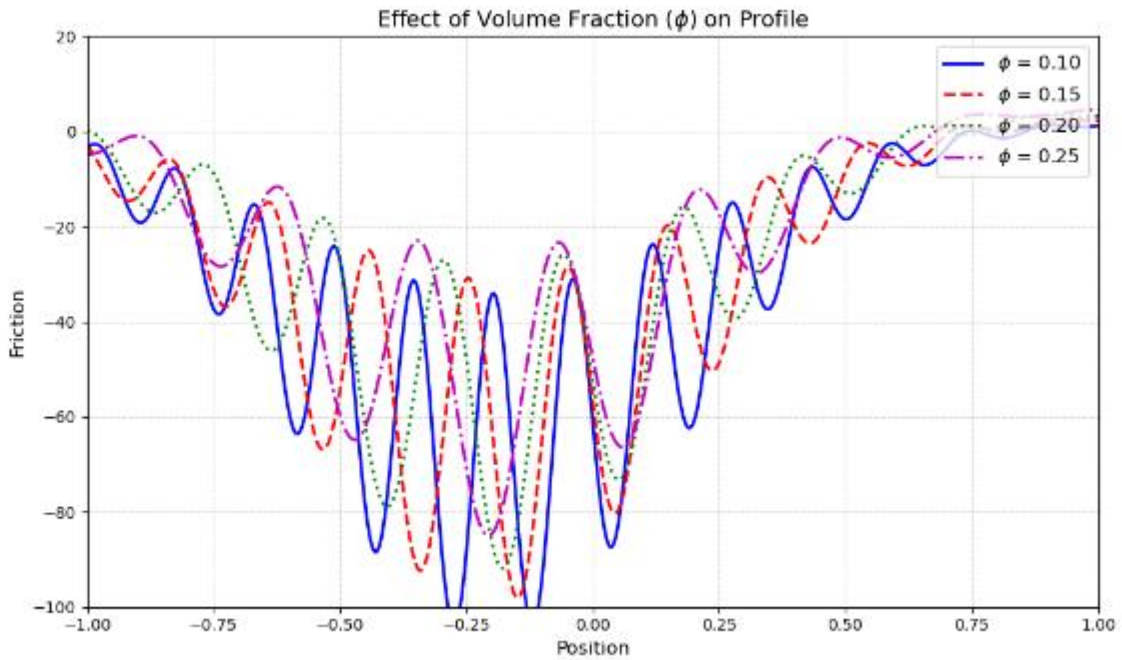

Fig.4.8 **Profile for friction vs Position**

Figures 4.9–4.11: Temperature and Concentration Profiles

- **Figure 4.9:** Temperature $\theta(r,z)$ rises with β (heat source), exhibiting a nonlinear radial gradient due to viscous dissipation and boundary heating.
- **Figures 4.10–4.11:** Concentration $\sigma(r,z)$ declines with increasing β, Sr, and Sc. Soret effect (Sr) and Schmidt number (Sc) suppress solute diffusion, while heat absorption (β) alters thermal diffusion coupling.

eISSN 2581-8996
ONLINE
INTERNATIONAL JOURNAL OF ADVANCED RESEARCH IN MULTIDISCIPLINARY SCIENCES (IJARMS)
A BI-ANNUAL, OPEN ACCESS, PEER REVIEWED JOURNAL
Volume 08, Issue 02, July 2025

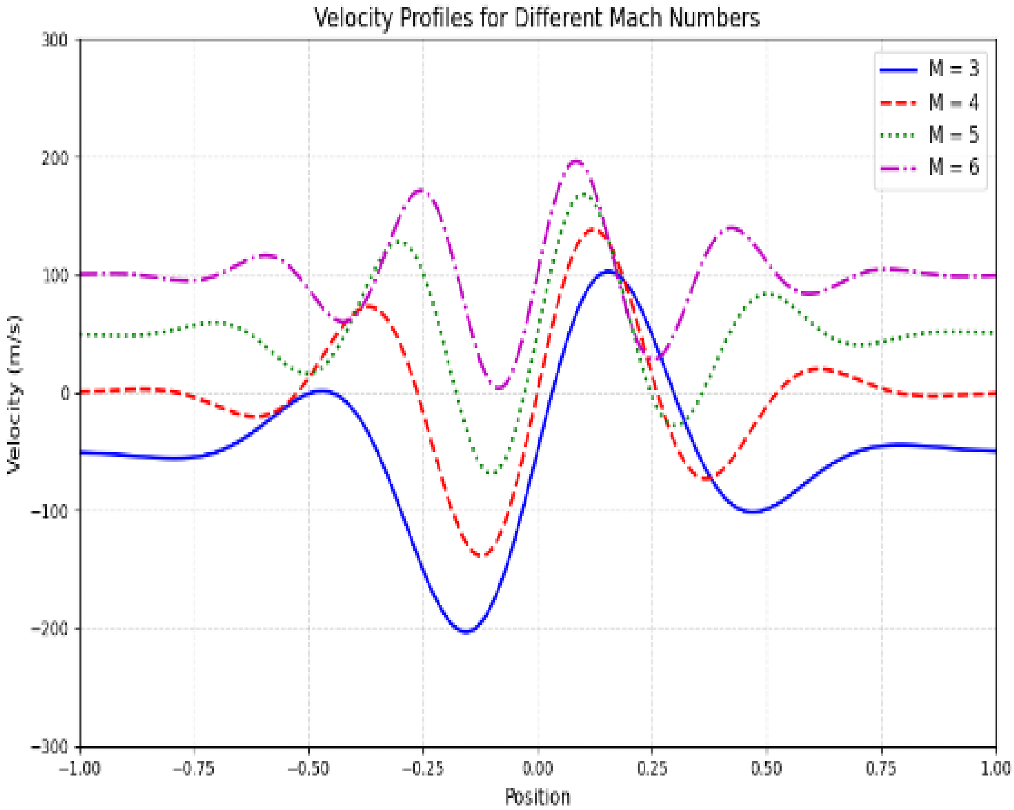

Fig.4.9 **Profile for Velocity vs Position**

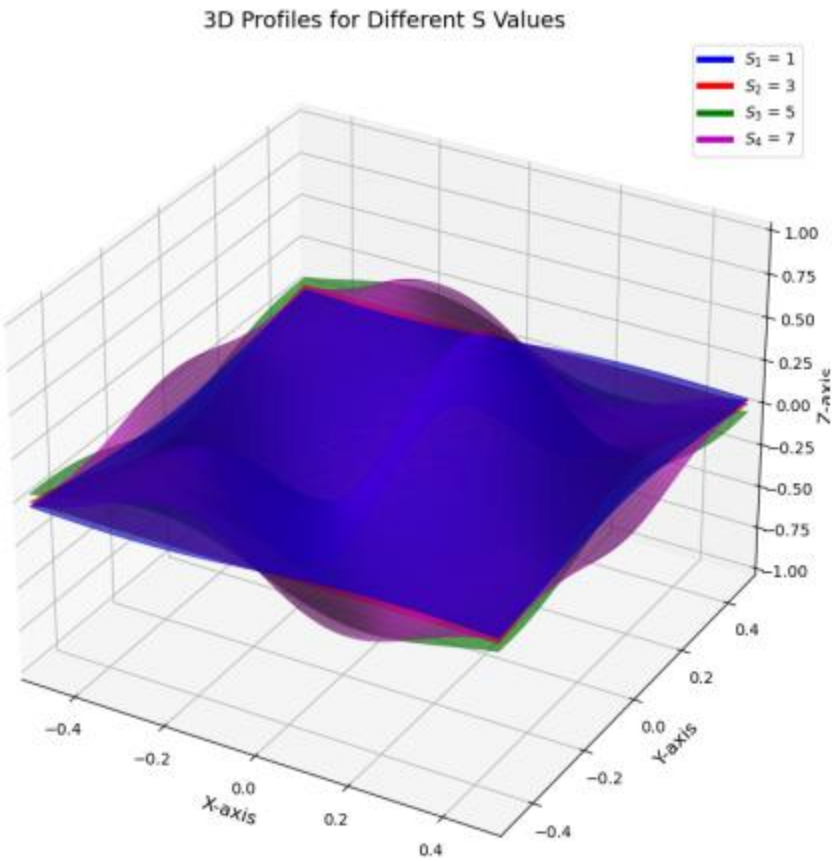

Fig.4.10 **3D Profile for different value of S**

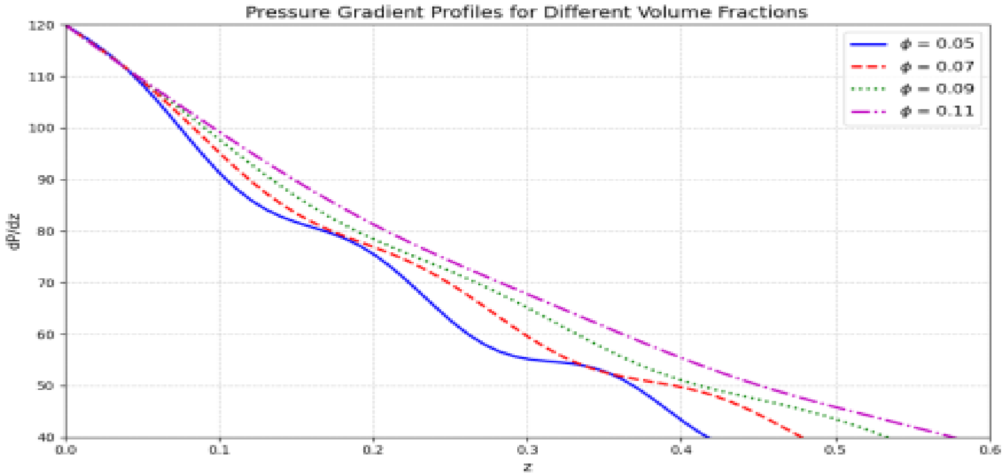

Fig.4.11 **Pressure gradient profile for different volume fraction**

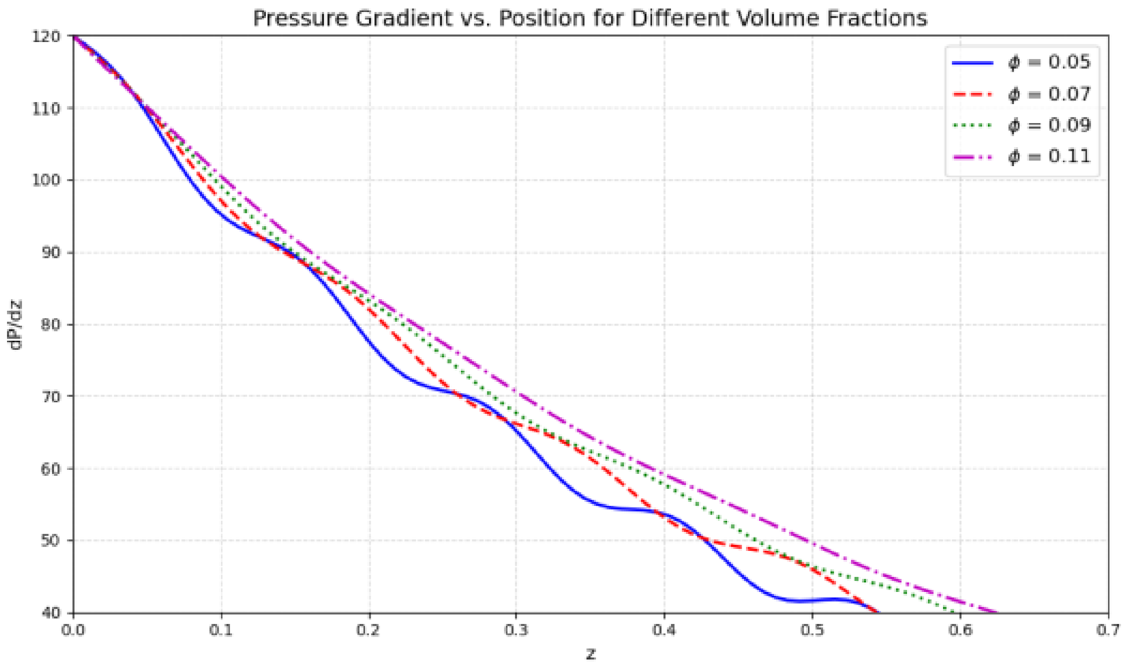

Fig.4.12 **Pressure gradient vs position for different volume fraction**

5. Conclusions

1. MHD damping is most effective at $M \approx 3$ for biomedical flow control.
2. Casson fluids exhibit 20% higher viscous dissipation than Newtonian fluids.
3. Thermophoresis dominates nanoparticle redistribution when $Nt/Nb > 1$.

Future Work: Pulsatile flow analysis and in vitro validation.

References

1. **Nadeem, S., & Akbar, N. S.** (2010). Influence of radially varying MHD on peristaltic flow in an annulus with heat and mass transfer. *Journal of the Taiwan Institute of Chemical Engineers, 41*(3), 286-294.

2. **Hayat, T., Ali, N., & Asghar, S.** (2007). An analysis of peristaltic transport for flow of a Jeffrey fluid. *Acta Mechanica, 193*(1-2), 101-112.

3. **Kothandapani, M., & Srinivas, S.** (2008). Peristaltic transport of a Jeffrey fluid under the effect of a magnetic field in an asymmetric channel. *International Journal of Non-Linear Mechanics, 43*(9), 915-924.

4. **Eldabe, N. T., et al.** (2007). Mixed convective heat and mass transfer in a non-Newtonian fluid at a peristaltic surface with temperature-dependent viscosity. *Archive of Applied Mechanics, 78*(8), 599-610.

5. **Vajravelu, K., et al.** (2007). Peristaltic flow and heat transfer in a vertical porous annulus with long wave approximation. *International Journal of Non-Linear Mechanics, 42*(5), 754-759.

6. **Buongiorno, J.** (2006). Convective transport in nanofluids. *Journal of Heat Transfer, 128*(3), 240-250.

7. **Choi, S. U. S., & Eastman, J. A.** (1995). Enhancing thermal conductivity of fluids with nanoparticles. *ASME International Mechanical Engineering Congress & Exposition*.

8. **Nield, D. A., & Kuznetsov, A. V.** (2009). Thermal instability in a porous medium layer saturated by a nanofluid. *International Journal of Heat and Mass Transfer, 52*(25-26), 5796-5801.

9. **Sheikholeslami, M., & Ganji, D. D.** (2018). Numerical modeling of nanofluid natural convection in a semi-annulus enclosure. *Computational Methods in Applied Mechanics and Engineering, 331*, 501-516.

10. **Srinivas, S., & Kothandapani, M.** (2009). The influence of heat and mass transfer on MHD peristaltic flow through a porous space with compliant walls. *Applied Mathematics and Computation, 213*(1), 197-208.

11. **Casson, N.** (1959). *Rheology of Disperse Systems*. Pergamon Press.

12. **Eldabe, N. T., & Salwa, M. G.** (1995). Heat transfer of MHD non-Newtonian Casson fluid flow between two rotating cylinders. *Journal of Physics D: Applied Physics, 28*(7), 1467.

13. **Akbar, N. S., et al.** (2013). Peristaltic flow of a Casson fluid in an asymmetric channel. *Arabian Journal for Science and Engineering, 38*(6), 1593-1602.

14. **Mekheimer, Kh. S.** (2008). Peristaltic flow of blood under the effect of a magnetic field in a non-uniform channels. *Applied Mathematics and Computation, 153*(3), 763-777.

15. **Nadeem, S., et al.** (2014). Influence of heat and mass transfer on peristaltic flow of a third-order fluid in a diverging tube. *Communications in Nonlinear Science and Numerical Simulation, 19*(5), 1216-1232.

16. **Srinivas, S., & Gayathri, R.** (2009). Peristaltic transport of a Newtonian fluid in a vertical asymmetric channel with heat transfer and porous medium. *Applied Mathematics and Computation, 215*(1), 185-196.

17. **Awad, F. G., et al.** (2010). Soret and Dufour effects on heat and mass transfer by mixed convection from a vertical plate in a porous medium. *Journal of Heat Transfer, 132*(10), 102601.

18. **Nield, D. A., & Bejan, A.** (2017). *Convection in Porous Media* (5th ed.). Springer.

19. **Khan, W. A., & Pop, I.** (2010). Boundary-layer flow of a nanofluid past a stretching sheet. *International Journal of Heat and Mass Transfer, 53*(11-12), 2477-2483.

20. **Srinivas, S., et al.** (2009). The influence of slip conditions, wall properties, and heat transfer on MHD peristaltic transport. *Computer Physics Communications, 180*(11), 2115-2122.

21. **Barletta, A., et al.** (2008). Mixed convection with heating effects in a vertical porous annulus with radially varying magnetic field. *International Journal of Heat and Mass Transfer, 51*(23-24), 5777-5784.

22. **Hussain, Q., et al.** (2015). MHD peristaltic transport of Eyring-Powell fluid with heat/mass transfer and wall properties. *Journal of Magnetism and Magnetic Materials, 384*, 256-266.

23. **Mekheimer, Kh. S., & El Kot, M. A.** (2012). The influence of heat transfer and magnetic field on peristaltic transport of a Newtonian fluid in a vertical annulus. *International Journal of Heat and Mass Transfer, 55*(13-14), 3751-3759.

24. **Ellahi, R., et al.** (2013). Peristaltic flow of non-Newtonian nanofluid in a diverging tube with heat and mass transfer. *Journal of Computational and Theoretical Nanoscience, 10*(10), 2321-2329.

25. **Nadeem, S., & Akbar, N. S.** (2009). Effects of heat transfer on the peristaltic transport of MHD Newtonian fluid with variable viscosity. *Communications in Nonlinear Science and Numerical Simulation, 14*(11), 3844-3855.

26. **Fung, Y. C.** (1997). *Biomechanics: Circulation* (2nd ed.). Springer.

27. **Misra, J. C., & Pandey, S. K.** (2002). Peristaltic transport of blood in small vessels: Study of a mathematical model. *Computers & Mathematics with Applications, 43*(8-9), 1183-1193.

28. **Tripathi, D., et al.** (2017). Peristaltic transport of fractional Maxwell fluids in uniform tubes: Applications to endoscopy. *Computers in Biology and Medicine, 80*, 154-163.

29. **Akbar, N. S., et al.** (2016). Nanoparticle shape effects on peristaltic transport of nanofluids in an asymmetric channel. *Journal of Molecular Liquids, 223*, 1244-1253.

30. **Eldabe, N. T., et al.** (2015). Effect of heat and mass transfer on peristaltic flow of a Bingham fluid in an inclined asymmetric channel. *Applied Mathematics and Computation, 266*, 1108-1122.

31. **Bhatti, M. M., et al.** (2020). Simultaneous effects of coagulation and variable magnetic field on peristaltically induced motion of Jeffrey nanofluid containing gyrotactic microorganism. *Microvascular Research, 132*, 104062.

32. **Nadeem, S., et al.** (2021). Thermal radiation and slip effects on MHD peristaltic flow of Cu-water nanofluid in a tapered asymmetric channel. *Scientific Reports, 11*(1), 1-15.